

Structure Formation in the Early Universe

Naoki Yoshida,¹

¹Institute for the Physics and Mathematics of the Universe,
University of Tokyo
5-1-5 Kashiwanoha, Kashiwa, Chiba 277-8568, Japan

*To whom correspondence should be addressed; E-mail: naoki.yoshida@ipmu.jp

To appear in Advanced Science Letters, 2009

The standard theory of cosmic structure formation posits that the present-day rich structure of the Universe developed through gravitational amplification of tiny matter density fluctuations generated in its very early history. Recent observations of the cosmic microwave background, large-scale structure, and distant supernovae determined the energy content of the Universe and the basic statistics of the initial density field with great accuracy. It has become possible to make accurate predictions for the formation and nonlinear growth of structure from early to the present epochs. We review recent progress in the theory of structure formation in the universe. We focus on the formation of the first cosmological objects. Results from state-of-the-art numerical simulations are presented. Finally, we discuss prospects for future observations of the first generation of stars and galaxies.

– cosmology, star formation, dark matter –

1 Introduction: The Dark Ages

Rich structures in the universe we see today, such as galaxies and galaxy clusters, have developed over a very long time. Astronomical observations utilizing large ground-based telescopes discovered distant galaxies and quasars (1, 2) that were in place when the Universe was less than one billion years old. We can probe directly, although not completely, the evolution of the cosmic structure all the way from the present-day to such an early epoch. We can also observe the state of the Universe at an even earlier epoch, about 380,000 years after the Big Bang, as the cosmic microwave background (CMB). The anisotropies of CMB provide information on the *initial conditions* for the formation of all the structures. In between these two epochs lies the remaining frontier of astronomy, when the universe was about a few to several million years old. The epoch is called the cosmic Dark Ages (3).

Shortly after the cosmological recombination epoch when hydrogen atoms were formed and the CMB photons were last-scattered, the CMB shifted to infrared, and then the universe would have appeared completely dark to human eyes. A long time had to pass until the first stars were born, which illuminate the universe once again and terminate the Dark Ages. The first stars are thought to be the first sources of light, and also the first sources of heavy elements that enable the formation of ordinary stellar populations, planets, and ultimately, the emergence of life.

Over the past years, there have been a number of theoretical studies on the yet unrevealed era in the cosmic history. Perhaps the current particular fascination with such studies is owing to recent rapid progress in observational astronomy. Existing telescopes are already probing early epochs close to the end of the Dark Ages, and planned observational programs are aimed at detecting directly light from objects farther away.

In this article, we review recent progress in the theory of structure formation in the early universe. We focus on the formation of the first generation stars. Theoretical studies hold promise for revealing the detailed process of primordial star formation for two main reasons: (1) the initial conditions, as determined cosmologically, are well-established, so that statistically equivalent realizations of a standard model universe can be accurately generated, and (2) all the important basic physics such as gravitation, hydrodynamics, and atomic and molecular processes in a hydrogen-helium gas are understood. In principle, therefore, it is possible to make solid predictions for the formation of early structure and of the first stars in an expanding universe. We describe some key physical processes. Computer simulations are often used to tackle the nonlinear problems of structure formation. We show the results from large cosmological N -body hydrodynamic simulations.

2 Hierarchical structure formation and the first cosmological objects

We first describe generic hierarchical nature of structure formation in the standard cosmological model which is based on weakly-interacting Cold Dark Matter (CDM). The primordial density fluctuations predicted by popular inflationary universe models have very simple characteristics (4). They are described by a Gaussian random field, and have a nearly scale-invariant power spectrum $P(k) \propto k^n$ for wavenumber k with $n \sim 1$. The perturbations come into the horizon in the radiation-dominated and then in the matter-dominated epochs. The difference in the growth rate in these epochs results in a modified power spectrum (5). Effectively the slope of the power-spectrum changes slowly as a function of length scale, but the final shape is still simple and monotonic in CDM models. The CDM density fluctuations have progressively larger amplitudes on smaller length scales. Hence structure formation is expected to proceed in a “bottom-up” manner, with smaller

objects forming earlier.

It is useful to work with a properly defined mass variance to obtain the essence of hierarchical structure formation. The mass variance is defined as the root-mean square of mass density fluctuations within a sphere that contains mass M . It is given by a weighted integral of the power spectrum as

$$\sigma^2(M) = \frac{1}{2\pi^2} \int P(k)W^2(kR)k^2 dk, \quad (1)$$

where the top-hat window function is given by $W(x) = 3(\sin(x)/x^3 - \cos(x)/x^2)$. Let us define the threshold over-density for gravitational collapse at redshift z as

$$\delta_{\text{crit}}(z) = 1.686/D(z), \quad (2)$$

where $D(z)$ is the linear growth factor of perturbations to z . Fig. 1 show the variance and the collapse threshold at $z = 0, 5, 20$. At $z = 20$, the mass of a halo which corresponds to a $3\text{-}\sigma$ fluctuation is just about $10^6 M_\odot$. As shown later in section 3, this is the characteristic mass of the first objects in which the primordial gas can cool and condense by molecular hydrogen cooling.

The mass variance is sensitive to the shape of the initial power spectrum. For instance, in warm dark matter models in which the power spectrum has an exponential cut-off at the particle free-streaming scale, the corresponding mass variance at small mass scales is significantly reduced (6, 7). In such models, early structure formation is effectively delayed, and hence small nonlinear objects form later than in the CDM model. Thus the formation epoch of the first objects and hence the beginning of cosmic reionization have a direct link to the nature of dark matter and the shape of the primordial density fluctuations (8, 9, 10). We discuss this issue further in Section 4.

3 Formation of the first cosmological objects

The basics of the formation of nonlinear dark matter halos are easily understood; because of its hierarchical nature, dark matter halos form in essentially the same way regardless of mass and the formation epoch. Halos will form at all mass scales by gravitational instability from scale-free density fluctuations. The first 'dark' objects are well defined, and are indeed halos of a very small mass which is set by dark matter particles' initial free-streaming motion (11).

The formation of the first baryonic objects involves a number of physical processes, and so is much more complicated. Baryons can collapse in dark matter halos only if the radiative cooling time is shorter than the age of the universe (12). The study of the evolution of primordial gas in the early universe and the origin of the first baryonic objects has a long history (13, 14, 15). The emergence of the standard cosmological model has enabled us to ask more specific questions, such as *when did the first objects form*, and *what is the characteristic mass*?

Recent numerical simulations of early structure formation show that this process likely began as early as when the age of the universe is less than a million years (3, 16). In these simulations, dense, cold clouds of self-gravitating molecular gas develop in the inner regions of small dark halos and contract into proto-stellar objects with masses in the range $\sim 100 - 1000M_{\odot}$. Fig. 2 shows the projected gas distribution in a cosmological simulation that includes hydrodynamics and primordial gas chemistry (17). Star-forming gas clouds are found at the knots of filaments, resembling the large-scale structure of the universe, although actually much smaller in mass and size. This manifest the hierarchical nature of structure in the CDM universe.

Unlike the formation of dark matter halos which is solely governed by gravity, star

formation involves at least several major processes as follows. For star formation to begin in the early universe, a sufficient amount of cold dense gas must accumulate in a dark halo. The primordial gas cannot efficiently cool radiatively because atoms have excitation energies that are too high, and molecules, which have accessible rotational energies, are very rare. Trace amounts of molecular hydrogen (H_2) can form via a sequence of reactions,



H_2 molecules, once formed, can change their quantum rotational and vibrational levels and emit photons. This allows the gas to cool and eventually condense to form gas clouds.

The critical temperature for these processes to operate is found to be about 2000 K. We here follow Ref. (18) to derive this characteristic temperature. Consider a gas with particle number density n and temperature T . The ionization fraction $x = n[\text{H}^+]/n$ and the molecular fraction $f = n[\text{H}_2]/n$ evolve as

$$\dot{x} = -k_{\text{rec}} n x^2, \quad (5)$$

$$\dot{f} = k_{\text{form}} n (1 - x - 2f) x, \quad (6)$$

where k_{rec} is hydrogen recombination rate and k_{form} is the net formation rate of molecular hydrogen. Equation (5) simply describes the rate of hydrogen recombination, by which the ionization fraction decreases, and equation (6) gives the rate of H_2 formation determined mainly by the above reaction (4). Assuming the cloud density and temperature remain roughly constant in a virialized halo, and taking $1 - x - 2f \sim 1$ for a neutral cosmic primordial gas, we obtain solutions

$$x(t) = \frac{x_0}{1 + x_0 n k_{\text{rec}} t}, \quad (7)$$

$$f(t) = f_0 + \frac{k_{\text{form}}}{k_{\text{rec}}} \ln(1 + x_0 n k_{\text{rec}} t). \quad (8)$$

Note the logarithmic dependence of f on time. Substituting the temperature dependence of the reaction rates $k_{\text{rec}}, k_{\text{form}}$, we obtain, after some straightforward algebra, a simple scaling of an asymptotic molecular fraction

$$f_c \propto T^{1.52}. \quad (9)$$

Remarkably, this simple scaling is shown to provide a rather accurate estimate. Fig. 3 shows the molecular fraction f_{H_2} against the virial temperature for halos located in a large cosmological simulation. The solid line is an analytical estimate of the H_2 fraction needed to cool the gas. It is computed from the cooling function of H_2 molecules (19). In Fig. 3, halos appear to be clearly separated into two populations; those in which the gas has cooled (solid circles), and the others (open circles). The analytic estimate yields a critical temperature of ~ 2000 K, which indeed agrees very well with the distribution of gas in the $f_{\text{H}_2} - T$ plane. There is an important dynamical effect, however. The gas in halos that accrete mass rapidly (primarily by mergers) is unable to cool efficiently owing to gravitational and gas dynamical heating. The effect explains the spread of halos into two populations at $T \sim 2000 - 5000$ K. Therefore, “minimum collapse mass” models are a poor characterization of primordial gas cooling and gas cloud formation in the hierarchical CDM model. The formation process is significantly affected by the dynamics of gravitational collapse. It is important to take into account the details of halo formation history (17, 20).

4 The role of dark matter and dark energy

The basic formation process of the first objects is described largely by the physics of a primordial gas. Its thermal and chemical evolution specifies a few important mass scales,

such as the Jeans mass at the onset of collapse (see Section 5). However, when and how primordial gas clouds are formed are critically affected by the particle properties of dark matter, by the shape and the amplitude of the initial density perturbations, and by the overall expansion history of the universe. We here introduce two illustrative examples; a model in which dark matter is assumed to be “warm”, and another cosmological model in which dark energy obeys a time-dependent equation of state.

If dark matter is warm, the matter power spectrum has an exponential cut-off at the particle free-streaming scale, and then the corresponding mass variance at small mass scales is significantly reduced (6, 7). The effect is clearly seen in Fig. 4. The gas distribution is much smoother in a model with warm dark matter. For the particular model with dark matter particle mass of 3 keV, dense gas clouds are formed in filamentary shapes, rather than in blobs embedded in dark matter halos (7, 21). While further evolution of the filamentary gas clouds is uncertain, it is expected that stars are lined up along filaments. Vigorous fragmentation of the filaments, if it occurs, can lead to the formation of multiple low-mass stars.

Dark matter particles might affect primordial star formation in a very different way. A popular candidate for dark matter is super-symmetric particles (22), neutralinos for instance. Neutralinos are predicted to have a large cross-section for pair-annihilation. Annihilation products are absorbed in a very dense gas clouds, which can counteract molecular cooling (23). Because primordial gas clouds are formed at the center of dark matter halos, where dark matter density is very large, the annihilation rate and resulting energy input can be significant. While the net effect of dark matter annihilation remains highly uncertain, it’d be interesting and even necessary to include the effect if neutralinos are detected in laboratories.

The nature of dark energy also affects the formation epoch of the first objects (24).

The growth rate of density perturbations is a function of cosmic expansion parameter, which is determined by the energy content of the universe. In general, the energy density of dark energy can be written as

$$\rho_{\text{DE}} \propto \exp \left[\int^a -3 \frac{da'}{a'} (1 + w(a')) \right], \quad (10)$$

where a is cosmic expansion parameter, and $w(a)$ defines the effective equation of state of dark energy via $P = w\rho$. For the simplest model of dark energy, i.e., Einstein's cosmological constant with $w = -1$, cosmic expansion is accelerated only at late epochs ($z < 1$), which is unimportant for early structure formation. However, some dark energy models predict time-dependent equation of state, which effectively shifts the formation epoch to early or later epochs. Fig. 5 shows the number of primordial gas clouds as a function of redshift for the standard Λ CDM model and for an evolving dark energy model.

Unfortunately, it is extremely difficult to measure the abundance of star-forming gas clouds as a function of time from currently available observations. It is possible to infer how early cosmic reionization began from the large-scale anisotropies of CMB polarization (25, 84), but the CMB polarization measurement does not put tight constraints on the reionization history. We will need to await for a long time until future radio observations map out the distribution of the intergalactic medium in the early universe by detecting redshifted 21cm emission from neutral hydrogen (26).

5 Formation of the first stars

Statistical properties of primordial star-forming clouds and the overall effect of cosmological bias have been studied in detail (17, 16, 27). We now describe more details of the formation process of stars – the first stars.

The dynamics of primordial gas cloud collapse has been studied extensively over the

past few decades (13,28). One-dimensional hydrodynamic simulations of spherical gas collapse were also performed with increasing levels of physics implementation (29,30). These studies showed that, while the overall evolution can be understood using a self-similar collapse model (31), there are clear differences in the thermal evolution of a primordial gas cloud from that of present-day, metal- and dust-enriched gas clouds. Three-dimensional cosmological simulations were performed by several groups so far (32,33). These calculations achieve a large dynamic range and implement primordial gas chemistry, and hence were able to follow the evolution of a primordial gas cloud in detail. They showed clearly how early gas clouds are formed in a cosmological context. However, the calculations are stopped at intermediate phases where the gas cloud is still gravitationally contracting.

Recently, an *ab initio* simulation of the formation of a primordial protostar has been finally performed (34). The simulation has an extraordinary spatial resolution, so that the highest gas densities reach “stellar” density, and thus it offers a detailed picture of how the first cosmological objects, protostars, form from primeval density fluctuations left over from the Big Bang. Unlike most simulations of star formation, the simulation does not assume any *a priori* equation of state for the gas. The thermal and chemical evolution is fully determined by molecular and atomic processes, including molecular hydrogen formation at both low and high densities, and transfer of molecular lines and continuum radiation. All of these processes are treated in a direct, self-consistent manner.

We describe in detail the simulation of Ref. (34), which followed the gravitational collapse of dark matter and the hydrodynamics of primordial gas. Small dark halos of about a half million solarmasses are assembled when the age of the universe is a few million years old. Through the action of radiative cooling, star-forming gas clouds collect in their host dark halo. Fig. 6 shows the projected gas density in and around the prestellar gas cloud. Note that the figures were made from a single simulation which covers a very

large dynamic range of $\sim 10^{13}$ in length scale. We see substantial variations in density and temperature even in the innermost 10 solar-radii region around the newly formed protostar.

Through a number of atomic and molecular processes, the cloud contract roughly isothermally; the density increases over 20 decades, but the temperature increase only by a factor of 10. When the central density reaches $n \sim 10^{18} \text{ cm}^{-3}$, the gas becomes completely optically thick to continuum radiation, and radiative cooling does not operate efficiently any more. Because the cloud core had initially a small angular momentum, the central part flattens to form a disk-like structure at this point. Further collapse and the associated dynamical heating triggers full-scale dissociation of hydrogen molecules in the central part. Thereafter, the gas cannot lose its thermal energy neither radiatively nor by dissociating molecules. The gas then contracts adiabatically, and its temperature quickly increases above several thousand Kelvin, while the density reaches $n \sim 10^{20} \text{ cm}^{-3}$. The contraction of the central part now becomes very slow, and hydrodynamic shocks are generated at the surface where supersonic gas infall is suddenly stopped. This is the moment of birth of a protostar. The protostar has a mass of just 0.01 solar masses. It has a radius of $\sim 5 \times 10^{11} \text{ cm}$ at its formation. The small mass is expected from the Jeans mass at the final adiabatic phase. The central particle number density of the protostar is $\sim 10^{21} \text{ cm}^{-3}$ and the temperature is well above 10,000 Kelvin.

A long standing question is whether or not a primordial gas cloud experiences vigorous fragmentation during its evolution (36, 37). Cosmological simulations performed so far showed consistently that a single small proto-stellar core is formed first (32, 34). It appears that gas cloud fragmentation does not occur. The so-called chemo-thermal instability has been studied in detail. The results from a semi-analytic calculation (38) and from direct three-dimensional simulations (35, 34) show that, at all evolutionary phases, the locally

estimated growth time for perturbations is longer than, or only comparable to, the local dynamical time for collapse. Hence, the cloud core does not fragment into multiple clumps by chemo-thermal instability, but instead its collapse is accelerated. Fragmentation of the cloud during later proto-stellar evolution has been examined (40, 41). Intriguingly, it was shown that a bar or a disk structure can become unstable to yield binary or multiple systems. This is an important issue to be explored further by three-dimensional simulations. The role of angular momentum and its transfer, and the radiative feedback effects from the central protostar(s) need to be studied.

On the assumption that there is only one stellar seed (protostar) at the center of the parent gas cloud, the subsequent protostellar evolution can be calculated using the standard model of star formation (39, 42, 43). For a very large accretion rate characteristic for a primordial gas cloud, $\dot{M} > 10^{-3} M_{\odot} \text{ yr}^{-1}$, a protostar can grow quickly to become a massive star. Fig. 7 shows the evolution of proto-stellar radius and mass for such large accretion rates. The resulting mass when the star reaches the zero-age main sequence is as large as one hundred times that of the sun (43, 35).

Overall, the lack of vigorous fragmentation, the large gas mass accretion rate, and the lack of significant source of opacity (such as dust) provide favourable conditions for the formation of massive, even very massive, stars in the early universe (35, 44, 45). A remaining important question is whether or not, and how gas accretion is stopped. This question is directly related to the final mass of the first stars. A few mechanisms are suggested to act to stop gas accretion and terminate the growth of a protostar (44). Following the growth of a primordial protostar to the end of its evolution in a three-dimensional simulation will be the next frontier.

6 Feedback from the first stars

The birth and death of the first generation of stars have important implications for the thermal state and chemical properties of the intergalactic medium in the early universe. At the end of the Dark Ages, the neutral, chemically pristine gas was reionized by ultraviolet photons emitted from the first stars, but also enriched with heavy elements when these stars ended their lives as energetic supernovae. The importance of supernova explosions, for instance, can be easily appreciated by noting that only light elements were produced during the nucleosynthesis phase in the early universe. Chemical elements heavier than lithium are thus thought to be produced exclusively through stellar nucleosynthesis, and they must have been expelled by supernovae to account for various observations of high-redshift systems (46, 47).

Feedback from the first stars may have played a crucial role in the evolution of the intergalactic medium and (proto-)galaxy formation. A good summary of the feedback processes is found in Ref. (48). We here review two important effects, and highlight a few unsolved problems.

6.1 Radiative feedback

The first feedback effect we discuss is radiation from the first stars. First stars can cause both negative and positive – in terms of star-formation efficiency – feedback effects. Far-UV radiation dissociates molecular hydrogen via Lyman-Werner resonances (49, 50, 51), while UV photo-ionization heat up the surrounding gas. Photo-ionization also increases the ionization fraction, which in turn promote H_2 formation. Yet another radiative feedback effect is conceivable; X-rays can promote H_2 production by boosting the free electron fraction in distant regions (52, 53). It is not clear whether negative or positive feedback dominates in the early universe.

One-dimensional calculations (e.g. (54)) show consistently strong negative effects of FUV radiation. Fig. 8 shows the distance at which the H_2 dissociation time equals the free-fall time. Hydrogen molecules in gas clouds within a few tens parsecs are easily destroyed by a nearby massive star. Three dimensional simulations also confirm the result in the optically-thin limit (55). However, gas self-shielding (opacity effects) need to be taken into account for dense gas clouds. H_2 dissociation becomes ineffective for large column densities of $N_{\text{H}_2} > 10^{14} \text{ cm}^{-2}$ for an approximately stationary gas (56). In fact, small halos are *not* optically-thin and thus the gas at the center can be self-shielded against FUV radiations (17, 57). Because of complexities associated with the dynamics, chemistry and radiative transfer involved in early gas cloud formation, the strength of the radiative feedback still remains rather uncertain. Recent simulations (58, 59) generally suggest that FUV radiation does not completely suppress star-formation even for large intensities of $> 10^{-22} \text{ erg sec}^{-1} \text{ Hz cm}^{-2}$. Contrary to the naive implication of the negative feedback from FUV radiation, star-formation can possibly continue in early minihalos. In light of this, analytic and semi-analytic models need to be refined. It is intriguing that the 5-year WMAP data do not suggest a very large optical depth to Thomson scattering of CMB, perhaps constraining a large contribution to reionization from minihalos (60, 61).

If the formation of H_2 is strongly suppressed by a FUV background, star formation proceeds in a quite different manner. A primordial gas cloud cools and condenses nearly isothermally by atomic hydrogen cooling. If the gas cloud has initially a small angular momentum, it can collapse to form an intermediate mass black hole may be formed (62, 63). Such first blackholes might power small quasars. X-ray from early quasars is suggested as a source of positive feedback effect by increasing the ionization fraction in a primordial gas (53). However, the net effect is much weaker than one naively expects from simple analytic estimates unless the negative feedback by FUV radiation is absent (64).

Ionizing radiation causes much stronger effects, at least locally. The formation of early HII regions were studied by a few groups using radiation hydrodynamics simulations (65, 66). Early HII regions are different from present-day HII regions in two aspects. Firstly, the first stars and their host gas cloud are hosted by a dark matter halo. Gravitational force exerted by dark matter needs to be included in the dynamics of early HII regions. Secondly, the *initial* gas density profile around the first star is typically steep (32, 35, 34). These two conditions make the evolution different from that of present-day local HII regions.

Fig. 9 shows the radial profiles of various quantities in and around an early HII region (67). The star-forming region is located as a dense molecular gas cloud within a small mass ($\sim 10^6 M_\odot$) dark matter halo. A single massive Population III star with $M_* = 100 M_\odot$ is embedded at the center. The formation of the HII region is characterized by initial slow expansion of an ionization front (I-front) near the center, followed by rapid propagation of the I-front throughout the outer gas envelope. The transition between the two phases determines a critical condition for the complete ionization of the halo. For small mass halos, the transition takes place within a few 10^5 years, and the I-front expands over the halo's virial radius (Fig. 9). The gas in the halo is effectively evacuated by a supersonic shock, with the mean gas density decreasing to $\sim 1 \text{cm}^{-3}$ in a few million years. It takes over tens to a hundred million years for the evacuated gas to be re-incorporated in the halo (68). The most important implication from this result is that star-formation in the early universe would be intermittent. Small mass halos can not sustain continuous star-formation.

Early gas clouds are expected to be strongly clustered (16, 20). Because even a single massive star affects over a kilo parsec volume, the mutual interactions between nearby star-forming gas clouds may be important. Large-scale cosmological simulations with the

radiative feedback effects such as those discussed here are clearly needed to fully explore the impact of early star formation.

6.2 Mechanical feedback

Massive stars end their lives as supernovae. Such energetic explosions in the early universe are thought to be violently destructive; they expel the ambient gas out of the gravitational potential well of small-mass dark matter halos, causing an almost complete evacuation (69, 70, 71, 72, 73). Since massive stars process a substantial fraction of their mass into heavy elements, SN explosions can cause prompt chemical enrichment, at least locally. It may even provide an efficient mechanism to pollute the surrounding intergalactic medium to an appreciable degree (74, 75).

Population III supernova explosions in the early universe were also suggested as a trigger of star-formation (76), but modern numerical simulations have shown that the expelled gas by supernovae falls back to the dark halo potential well after about the system's free-fall time (75, 77). The density and density profile around the supernova sites are of particular importance because the efficiency of cooling of supernova remnants is critically determined by the density inside the blastwave. If the halo gas is evacuated by radiative feedback prior to explosion, the supernova blastwave propagates over the halo's virial radius, leading to complete evacuation of the gas even with the input energy of 10^{51} erg. A large fraction of the remnant's thermal energy is lost in $10^5 - 10^7$ yr by line cooling, whereas, for even greater explosion energies, the remnant cools mainly via inverse Compton scattering. The situation is clearly different from the local galactic supernova. In the early universe, the inverse Compton process with cosmic background photons acts as an efficient cooling process.

Fig. 11 summarizes the results from a series of calculations of Ref. (73). It shows the

destruction efficiency by a single SN explosion for a wide range of explosion energy and host halo mass. A simple criterion, $E_{\text{SN}} > E_{\text{bi}}$, where E_{bi} is the gravitational binding energy, is often used to determine the destruction efficiency. However, whether or not the halo gas is effectively blown-away is determined not only by the host halo mass (which gives an estimate of E_{bi}), but also by a complex interplay of hydrodynamics and radiative processes. SNRs in dense environments are highly radiative and thus a large fraction of the explosion energy can be quickly radiated away. An immediate implication from the result is that, in order for the processed metals to be transported out of the halo and distributed to the IGM, I-front propagation and pre-evacuation of the gas must precede the supernova explosion. This roughly limits the mass of host halos from which metals can be ejected into the IGM to $< 10^7 M_{\odot}$, i.e., the first generation of stars can be a significant source of early metal-enrichment of the IGM (69, 75, 72).

Although metal-enrichment by the first supernovae could greatly enhance the gas cooling efficiency, which might possibly change the mode of star-formation to that dominated by low-mass stars (78), the onset of this ‘second-generation’ stars may be delayed owing to gas evacuation, particularly in low-mass halos. This again supports the notion that early star-formation is likely self-regulating. If the first stars are massive, only one period of star-formation is possible for a small halo and its descendants within a Hubble time. The sharp decline in the destruction efficiency at $M_{\text{halo}} > 10^7 M_{\odot}$ (see Fig. 11) indicates that the global cosmic star formation activity increases only after a number of large mass ($> 10^{7-8} M_{\odot}$) halos are assembled.

7 Toward the formation of the first galaxies

The hierarchical nature of cosmic structure formation (see Section 2) naturally predicts that stars or stellar size objects form first, earlier than galaxies form. The first generation

of stars set the scene for the subsequent galaxy formation. The characteristic minimum mass of a first galaxy (including dark matter) is perhaps $\sim 10^7 - 10^8 M_\odot$, in which the gas heated up to $10^4 - 10^5$ Kelvin by the first star feedback can be retained.

The first galaxies are assembled through a number of large and small mergers, and then turbulence is generated dynamically, which likely changes star-formation process from a quiescent one (like in minihalos) to a highly complicated but organized one. There have been a few attempts to directly simulate this process in a cosmological context (81, 82). The results generally argue that star-formation in the large mass system is still an inefficient process overall. However, a significant difference is that the inter-stellar medium is likely metal-enriched in the first galaxies. Theoretical calculations (79, 80) show that cooling by heavy elements and by dust can bring the gas temperature at the onset of run-away collapse substantially lower than for a primordial gas. The lower gas temperature causes two effects; it lowers the Jeans mass ($\propto T^{3/2}/\rho^{1/2}$), and also lowers the mass accretion rate ($\propto c_s^3/G$), thereby providing at least two necessary conditions for low-mass star-formation. Combined effects of strong turbulence and metal-enrichment might make the stellar initial mass function be close to that in the present-day star-forming regions.

Understanding the formation of the first galaxies is much challenging, because of the complexities described above. Nevertheless it is definitely the subject where theoretical models can be really tested against direct observations in the near future. The first galaxies may be more appropriately called faint proto-galaxies, and will be detected by the next generation telescopes. *JWST* will measure the luminosity function of faint galaxies at $z > 7$, which reflects the strength of feedback effects from the first stars (83).

8 Prospects for future observations

A number of observational programs are planned to detect the first stars and galaxies, both directly and indirectly. We close this review by discussing prospects for future observations.

The first galaxies will be the main target of next generation (near-)infrared telescopes, while indirect information on the first stars will be obtained from the CMB polarization, the near-infrared background, high-redshift supernovae and gamma-ray bursts, and from the so-called Galactic archeology.

The five-year data of the *Wilkinson Microwave Anisotropy Probe (WMAP)* yields the CMB optical depth to Thomson scattering, $\tau \simeq 0.09 \pm 0.03$ (84). This measurement provides an integral constraint on the total ionizing photon production at $z > 6$ (85). More accurate polarization measurements by *Planck* and by a continued operation of *WMAP* will further tighten the constraint on the reionization history of the universe, $x_e(z)$ (86). In a longer term, future radio observations such as *Square Kilometer Array* will map out the distribution of the intergalactic hydrogen in the early universe. The topology of reionization and its evolution will be probed (26).

The first stars in the universe are predicted to be massive, as discussed in this article, and so they are likely progenitors of energetic supernovae and associated GRBs at high redshifts (87). Infrared color can be utilized to identify supernovae at $z < 13$ (88). A realistic 1-year *JWST* survey will discover 1-30 supernovae at $z > 5$ (89). Gamma-ray bursts are the brightest explosions in the universe, and thus are detectable out to redshifts $z > 10$ in principle. Recently, *Swift* satellite has detected a GRB originating at $z > 6$ (89, 90), thus demonstrating the promise of GRBs as probes of the early universe.

Very metal-poor stars – the stellar relics – provide invaluable information on the

conditions under which these low-mass stars formed (*91, 92*). It is expected that the relics of early generation stars are orbiting near the centers of galaxies at the present epoch (*93*). While conventionally halo stars are surveyed to find very metal-poor stars, the APOGEE project is aimed at observing $\sim 100,000$ stars in the bulge of Milky Way (*94*). The nature of early metal-enrichment must be imprinted in the abundance patterns in the bulge stars.

Altogether, these observations will finally fill the gap in our knowledge on the history of the universe, and will end the “Dark Ages”.

The work is supported in part by the Grants-in-Aid for Young Scientists (S) 20674003 by the Japan Society for the Promotion of Science.

References

1. X. Fan et al., *Astronomical J.* **125**, 1649 (2003).
2. M. Iye et al., *Nature* **443**, 186 (2006).
3. J. Miralda-Escude, *Science* **300**, 1904 (2003).
4. D. H. D. Lyth & A. A. Riotto, *Physics Reports* **314**, 1 (1999).
5. S. Dodelson, *Modern Cosmology*, Academic Press, (2003).
6. R. Barkana, Z. Haiman, J. P. Ostriker, *Astrophys. J.* **558**, 482 (2001).
7. N. Yoshida, A. Sokasian, L. Hernquist, and V. Springel, *Astrophys. J.* **591**, L1 (2003)
8. A. Kosowsky & M. S. Turner, *Physical Review D* **52**, 1739 (1995)
9. R. S. Somerville, J. S. Bullock, and M. Livio, *Astrophys. J.*, **593**, 616 (2003)
10. N. Yoshida, A. Sokasian, L. Hernquist, and V. Springel, *Astrophys. J* **598**, 73 (2003)

11. J. Diemand, B. Moore, J. Stadel, *Nature* **433**, 389 (2005)
12. J. P. Ostriker and M. J. Rees, *M.N.R.A.S.* **179**, 541 (1977)
13. T. Matsuda, H. Sato, and H. Takeda, *Prog. Theor. Phys.* **41**, 840 (1969)
14. A. Kashlinsky & M. J. Rees, *M.N.R.A.S.* **205**, 21 (1983)
15. H. M. P. Couchman & M. J. Rees, *M.N.R.A.S.* **221**, 53 (1986)
16. L. Gao, N. Yoshida, T. Abel, C. S. Frenk, A. Jenkins, & V. Springel, *M.N.R.A.S.* **378**, 449 (2007)
17. N. Yoshida, T. Abel, L. Hernquist, and N. Sugiyama, *Astrophys. J.* **592**, 645 (2003)
18. M. Tegmark, J. Silk, M. J. Rees, A. Blanchard, T. Abel, and F. Palla, *Astrophys. J.* **474**, 1 (1997)
19. D. Galli & F. Palla, *Astron. Astrophys.* **335**, 403 (1998).
20. D. Reed, R. Bower, C. S. Frenk, A. Jenkins, T. Theuns, S. D. M. White, *M.N.R.A.S.* **363**, 393 (2005).
21. L. Gao & T. Theuns, *Science* **317**, 1527 (2007).
22. G. Jungman, M. Kamionkowski, K. Griest, *Physics Reports* **267**, 195 (1996).
23. D. Spolyar, K. Freese, P. Gondolo, *Phys. Rev. Lett.* **100**, 1101 (2008).
24. U. Maio, K. Dolag, M. Meneghetti, L. Moscardini, N. Yoshida, C. Baccigalupi, M. Bartelmann, & F. Perrota, *M.N.R.A.S* **373**, 869 (2006).
25. M. Zaldarriaga & U. Seljak, *Phys. REv. D* **55**, 1830 (1997)

26. P. R. Shapiro, K. Ahn, M. A. Alvarez, I. T. Iliev, H. Martel, & D. Ryu, *Astrophys. J.* **646**, 681 (2006)
27. B. W. O'Shea, M. L. Norman, *Astrophys. J.* **654**, 66 (2007)
28. F. Palla, E. E. Salpeter, S. W. Stahler, *Astrophys. J.* **52**, 155 (1983).
29. K. Omukai & R. Nishi, *Astrophys. J.* **508**, 141 (1998)
30. E. Ripamonti, F. Haardt, A. Ferrara, M. Colpi, *M.N.R.A.S.* **334**, 401 (2002).
31. R. B. Larson, *M.N.R.A.S.* **145**, 271 (1969).
32. T. Abel, G. L. Bryan, M. L. Norman, *Science* **295**, 93 (2002).
33. V. Bromm, P. S. Coppi, & R. B. Larson, *Astrophys. J.* **564**, 23 (2002)
34. N. Yoshida, K. Omukai, L. Hernquist, *Science* **321**, 669 (2008)
35. N. Yoshida, K. Omukai, L. Hernquist, T. Abel, *Astrophys. J.* **613**, 406 (2006).
36. Y. Sabano, & Y. Yoshii, *Pub. Astron. Soc. Jpn* **29**, 207 (1977)
37. J. Silk, *M.N.R.A.S.* **205**, 705 (1983)
38. K. Omukai, & Y. Yoshii, *Astrophys. J.* **599**, 746 (2003)
39. S. W. Stahler, F. Palla, & E. E. Salpeter, *Astrophys. J.* **302**, 590 (1986)
40. M. N. Machida, K. Omukai, T. Matsumoto, S. Inutsuka, *Astrophys. J.* **677**, 813 (2008).
41. P. C. Clark, S. C. O. Glover, R. S. Klessen, *Astrophys. J.* **672**, 757 (2008).
42. K. Omukai & F. Palla, *Astrophys. J.* **561**, 55 (2001).

43. K. Omukai & F. Palla, *Astrophys. J.* **589**, 677 (2003).
44. C. F. McKee & J. C. Tan, *Astrophys. J.* **681**, 771 (2008).
45. T. Ohkubo, H. Umeda, K. Nomoto, N. Yoshida, S. Tsuruta, *Astrophys. J.* submitted
46. F. Walter et al., *Nature* **424**, 406 (2003).
47. A. Songaila, *Astron. J.* **130**, 1996 (2005).
48. B. Ciardi, in *First Stars III* B. O'shea et al. eds. AIP publisher (2008)
49. T. P. Stecher & D. A. Williams, *Astrophys. J.* **149**, 29 (1967)
50. K. Omukai & R. Nishi, *Astrophys. J.* **518**, 64 (1999)
51. Z. Haiman, T. Abel & M. J. Rees, *Astrophys. J.* **534**, 11 (2000)
52. S.-P. Oh, *Astrophys. J.* **569**, 558 (2001)
53. M. Ricotti & J. P. Ostriker, *M.N.R.A.S.* **352**, 547 (2004)
54. S. C. O. Glover & P. W. J. L. Brand, *M.N.R.A.S.* **321**, 385 (2001)
55. M. E. Machacek, G. L. Bryan & T. Abel, *Astrophys. J.* **548**, 509 (2001)
56. B. Draine & F. Bertoldi, *Astrophys. J.* **468**, 269 (1996)
57. H. Susa, *Astrophys. J.* **659**, 908 (2007)
58. K. Ahn, *M.N.R.A.S.* **375**, 881 (2007)
59. B. W. O'Shea & M. L. Norman, *Astrophys. J.* **673**, 14 (2008)
60. M. A. Alvarez, P. R. Shapiro, K. Ahn, & I. T. Iliev, *Astrophys. J.* **644**, 101 (2006)

61. Z. Haiman & G. L. Bryan, *Astrophys. J.* **650**, 7 (2007)
62. V. Bromm & A. Loeb, *Astrophys. J.* **596**, 34 (2003)
63. K. Omukai, R. Schneider, & Z. Haiman, *Astrophys. J.* **686**, 801 (2008)
64. M. E. Machacek, G. L. Bryan & T. Abel, *M.N.R.A.S.* **338**, 273 (2003)
65. T. Kitayama, N. Yoshida, H. Susa, and M. Umemura, *Astrophys. J.* **613**, 631 (2004)
66. D. Whalen, T. Abel, and M. L. Norman, *Astrophys. J.* **610**, 14 (2004)
67. T. Abel, J. H. Wise, and G. L. Bryan, *Astrophys. J.* **659**, 87 (2007)
68. N. Yoshida, S.-P. Oh, T. Kitayama, & L. Hernquist, *Astrophys. J.* **663**, 687 (2007)
69. V. Bromm, N. Yoshida, & L. Hernquist, *Astrophys. J.* **596**, L135 (2003)
70. K. Wada & A. Venkatesan, *Astrophys. J.* **591**, L38 (2003)
71. T. Kitayama & N. Yoshida, *Astrophys. J.* **630**, 675
72. T. H. Greif, J. L. Johnson, R. S. Klessen, & V. Bromm, *Astrophys. J.* **670**, 1 (2007).
73. D. Whalen, B. van Veelen, B. W. O'Shea, M. L. Norman, *Astrophys. J.* **682**, 49 (2008)
74. M. Mori, A. Ferrara, & P. Madau, *Astrophys. J.* **571**, 40 (2002)
75. N. Yoshida, V. Bromm, & L. Hernquist, *Astrophys. J.* **605** 579 (2004)
76. B. Carr, J. R. Bond, & D. Arnett, *Astrophys. J.* **277**, 445 (1984)
77. J. L. Johnson & V. Bromm, *M.N.R.A.S.* **374**, 1557 (2007)
78. R. Schneider, K. Omukai, A. K. Inoue & A. Ferrara, *M.N.R.A.S.* **369**, 1437 (2006)

79. V. Bromm & A. Loeb, *Nature* **425**, 812 (2003)
80. K. Omukai, T. Tsuribe, R. Schneider, A. Ferrara, *Astrophys. J.* **667**, 117 (2005).
81. J. Wise & T. Abel, *Astrophys. J.* **665**, 899 (2007).
82. T. H. Greif, J. L. Johnson, R. S. Klessen, & V. Bromm, *M.N.R.A.S.* **387**, 1021 (2008).
83. Z. Haiman, in *Astrophysics in the Next Decade* Eds. H. Thronson et al., Springer Dordrecht (2008).
84. E. Komatsu et al., *Astrophys. J.* in press (2009)
85. L. Hui & Z. Haiman, *Astrophys. J.* **596**, 9 (2003)
86. G. P. Holder et al. *Astrophys. J.* **595**, 13 (2003)
87. S. E. Woosley & J. S. Bloom, *Annu. Rev. Astron. Astrophys.* **44**, 507 (2006)
88. A. Mesinger, B. Johnson, Z. Haiman, *Astrophys. J.* **637**, 80 (2006)
89. N. Kawai et al., *Nature* **440**, 184 (2006)
90. J. Greiner et al., *Astrophys. J.* in press
91. N. Christlieb *et al.*, *Nature* **419**, 904 (2002).
92. A. Frebel *et al.*, *Nature* **434**, 871 (2005).
93. White, S. D. M. & Springel, V., in *The First Stars*, A. Weiss eds., Springer-Verlag (2000)
94. <http://www.sdss3.org>

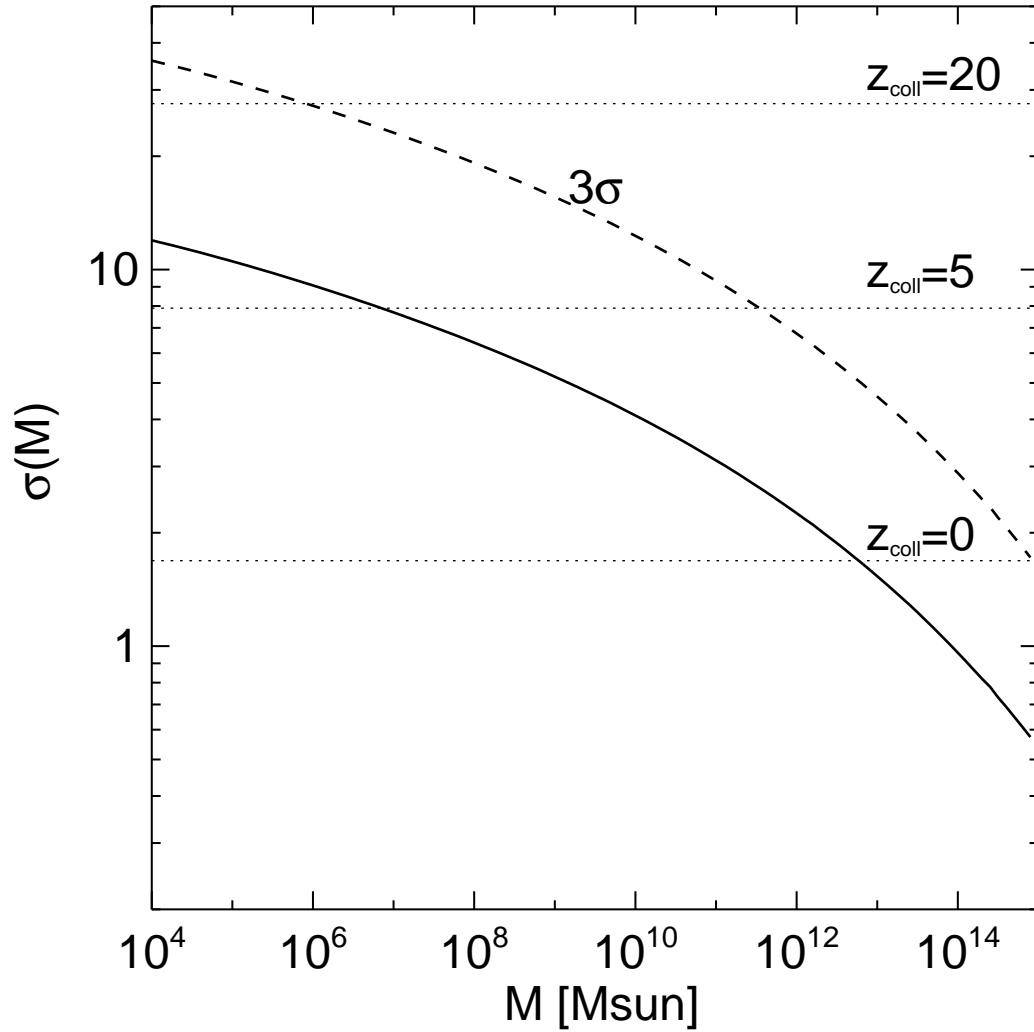


Figure 1: Mass variance and collapse thresholds for a flat CDM model with cosmological constant. The assumed cosmological parameters are, matter density $\Omega_m = 0.3$, baryon density $\Omega_b = 0.04$, amplitude of fluctuations $\sigma_8 = 0.9$, and the Hubble constant $H_0 = 70 \text{ km s}^{-1} \text{ Mpc}^{-1}$.

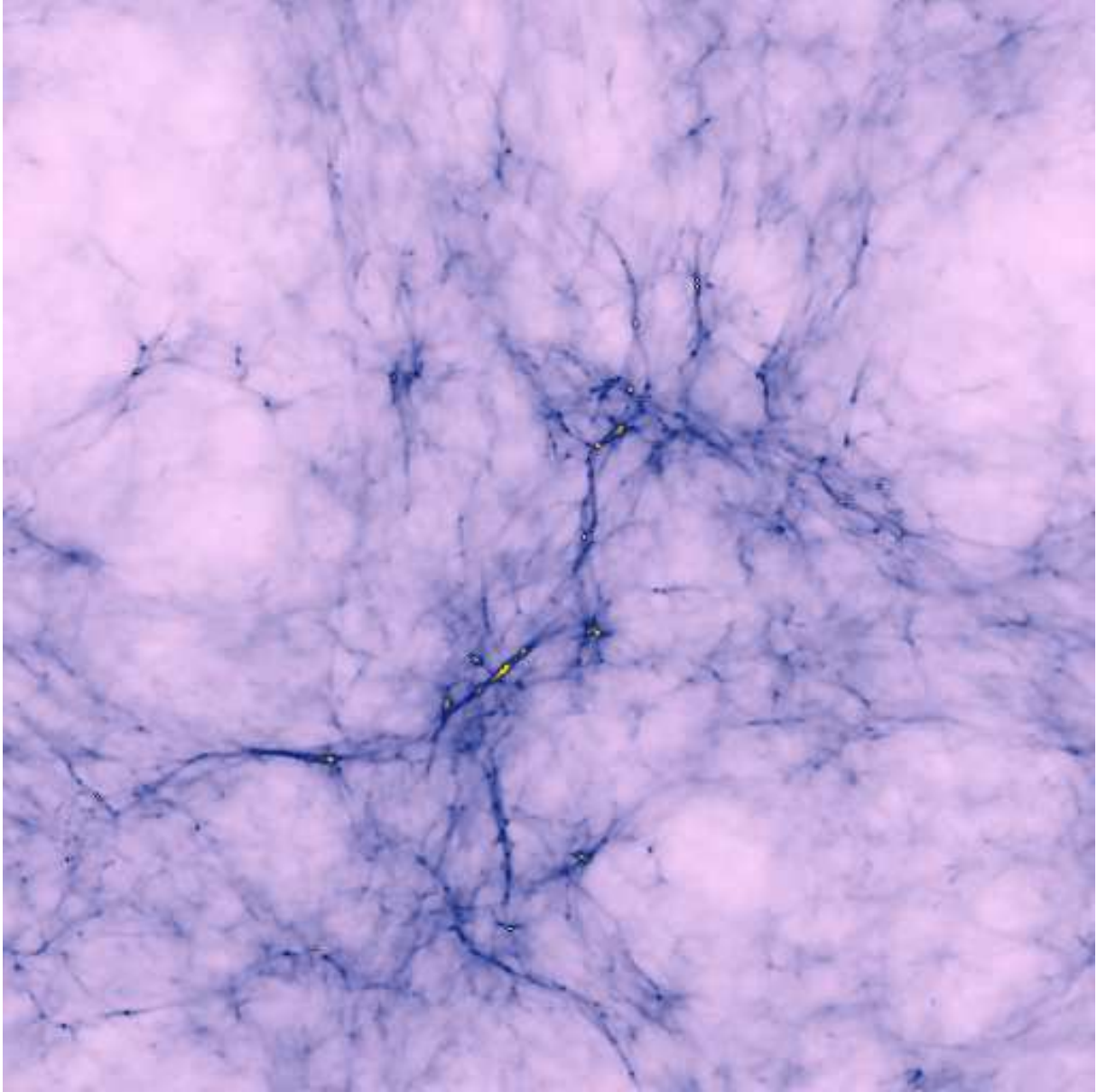


Figure 2: The projected gas distribution at $z = 17$ in a cubic volume of $600h^{-1}\text{kpc}$ on a side. The cooled dense gas clouds appear as bright spots at the intersections of the filamentary structures. From Ref. (17).

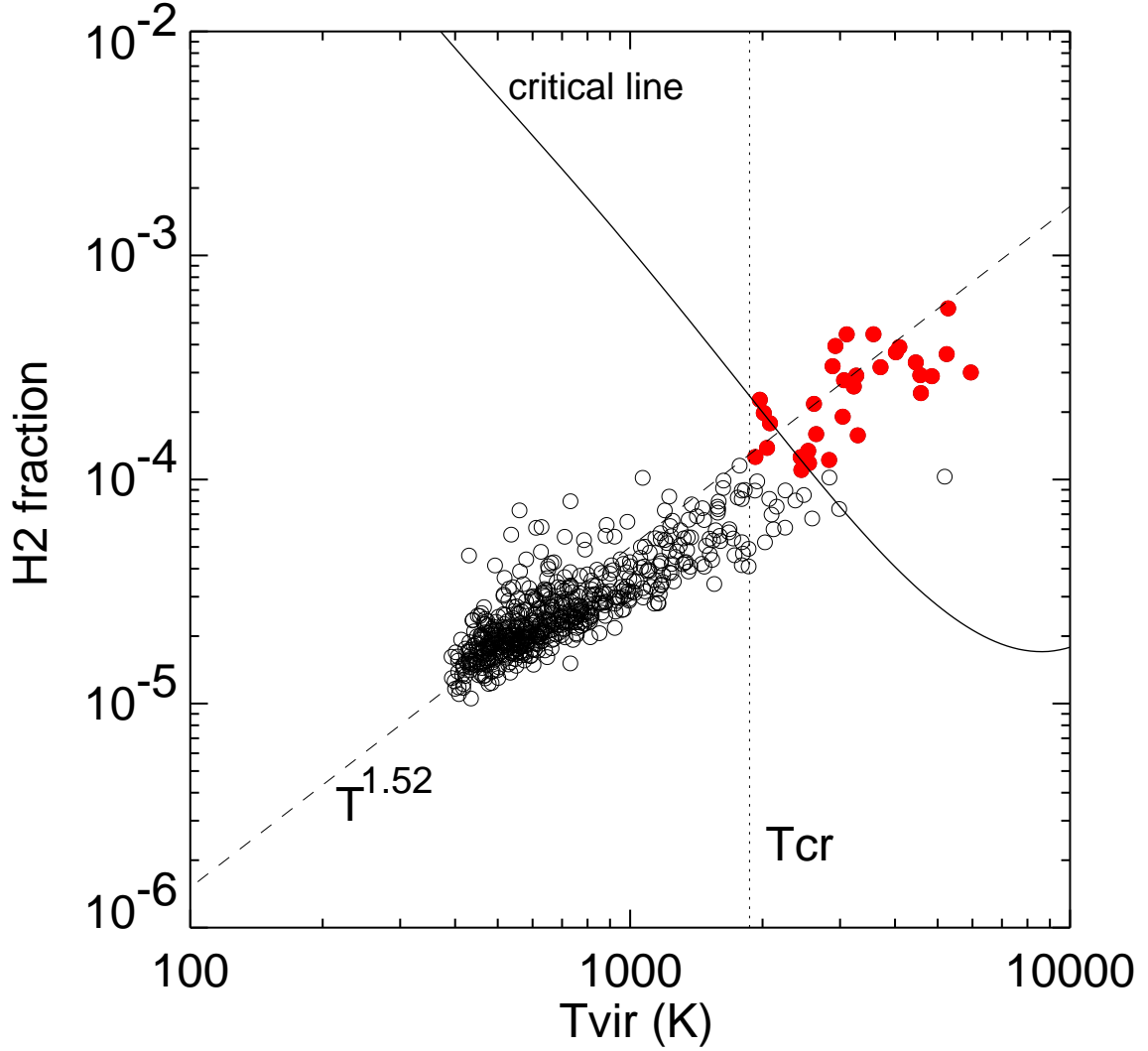


Figure 3: The mass weighted mean H₂ fraction versus virial temperature for the halos that host gas clouds (filled circles) and for those that do not (open circles) at $z = 17$ ($t_{\text{age}} = 300$ Myrs). The solid curve is the H₂ fraction needed to cool the gas at a given temperature and the dashed line is the asymptotic H₂ fraction (see equation [9]). From Ref. (17).

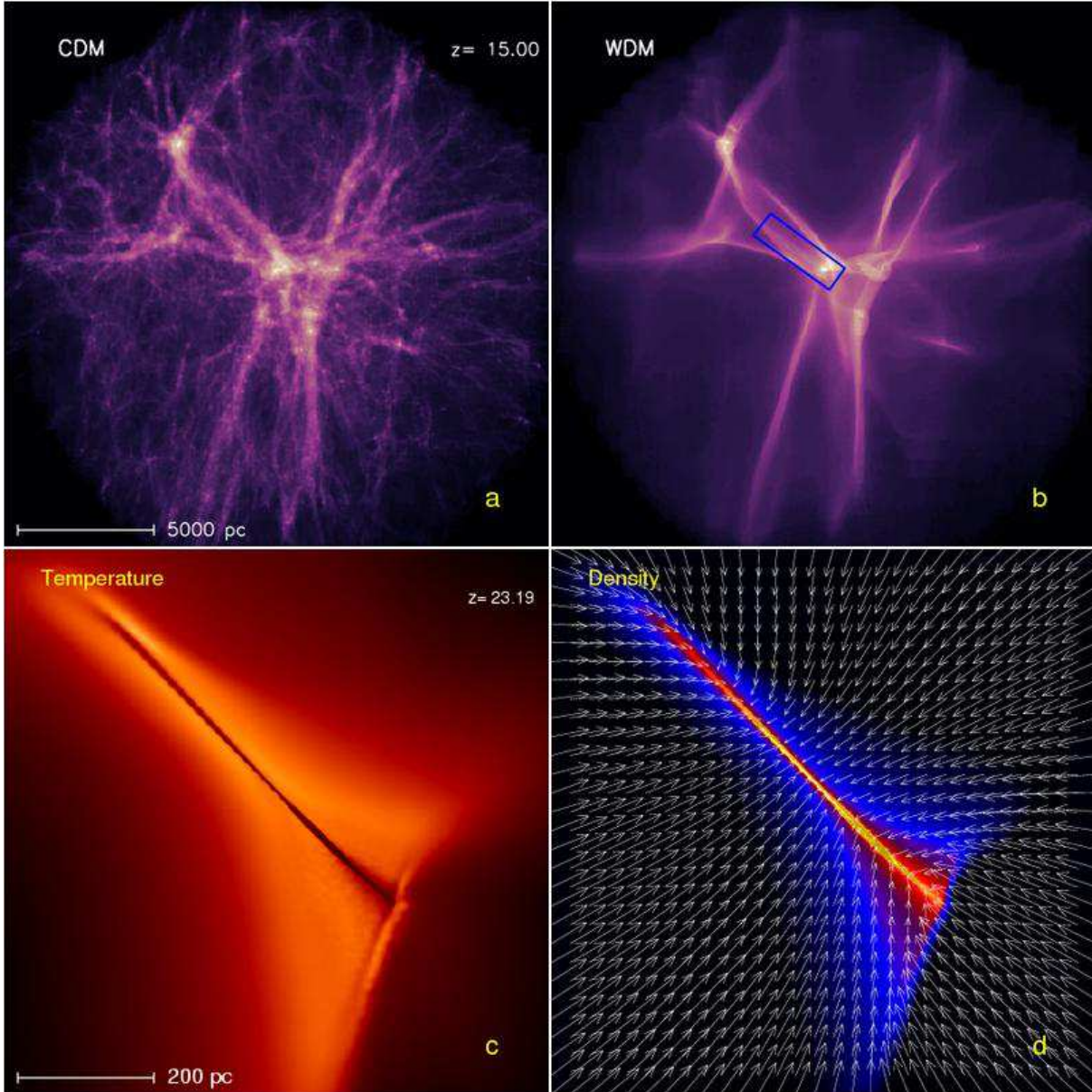


Figure 4: The projected gas distribution at $z = 15$ for the standard CDM model (left) and for a WDM model (right). We see much smoother matter distribution in the WDM model, in which gas clouds are formed in the prominent filamentary structure (bottom panels). From Gao & Theuns 2007, Science.

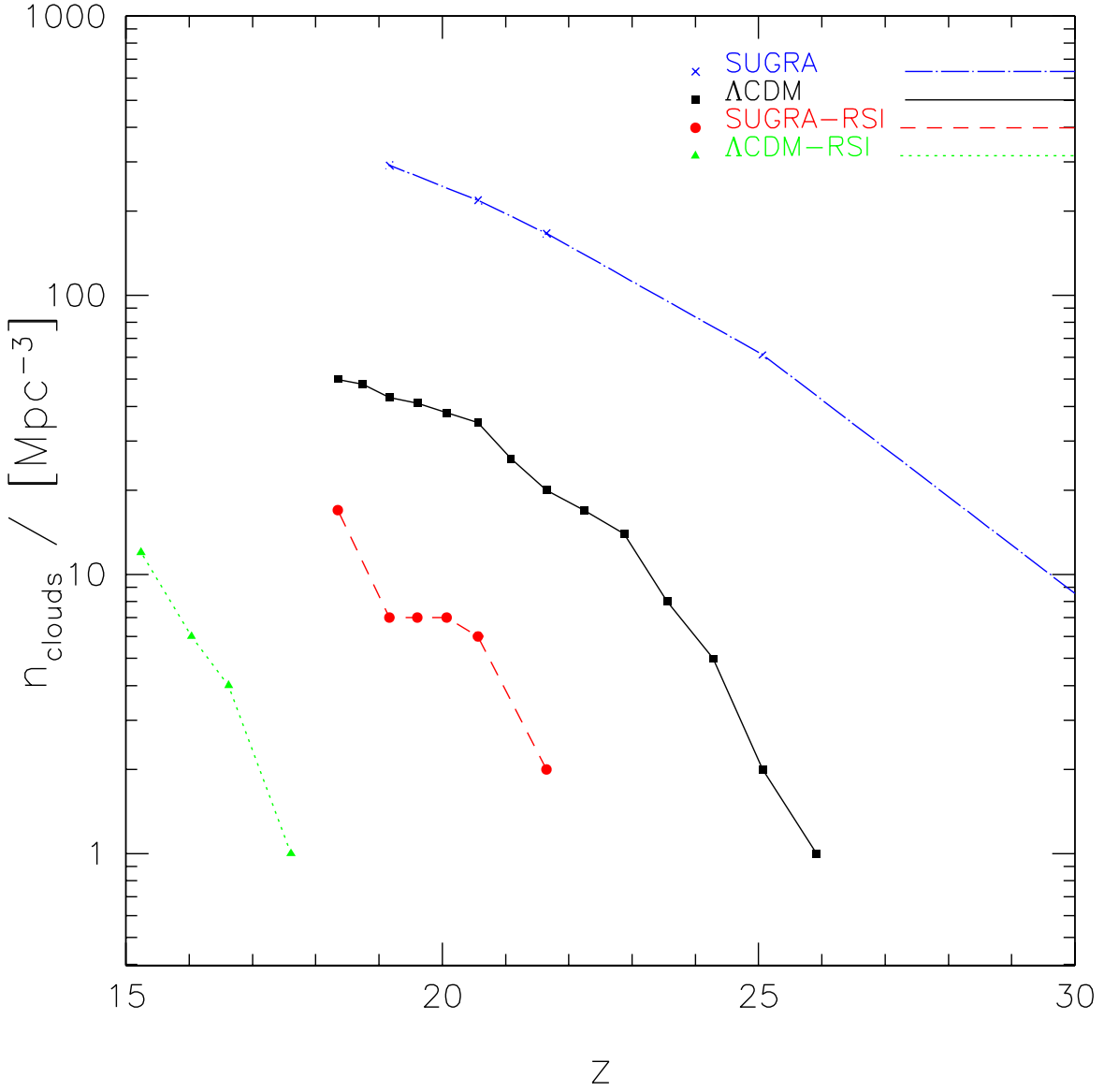


Figure 5: The number of primordial gas clouds at high redshifts for a variety of models; SUGRA (an evolving dark energy), Λ CDM, SUGRA + a running spectral inflation model, and Λ CDM + a running spectral inflation model. From Ref. (24).

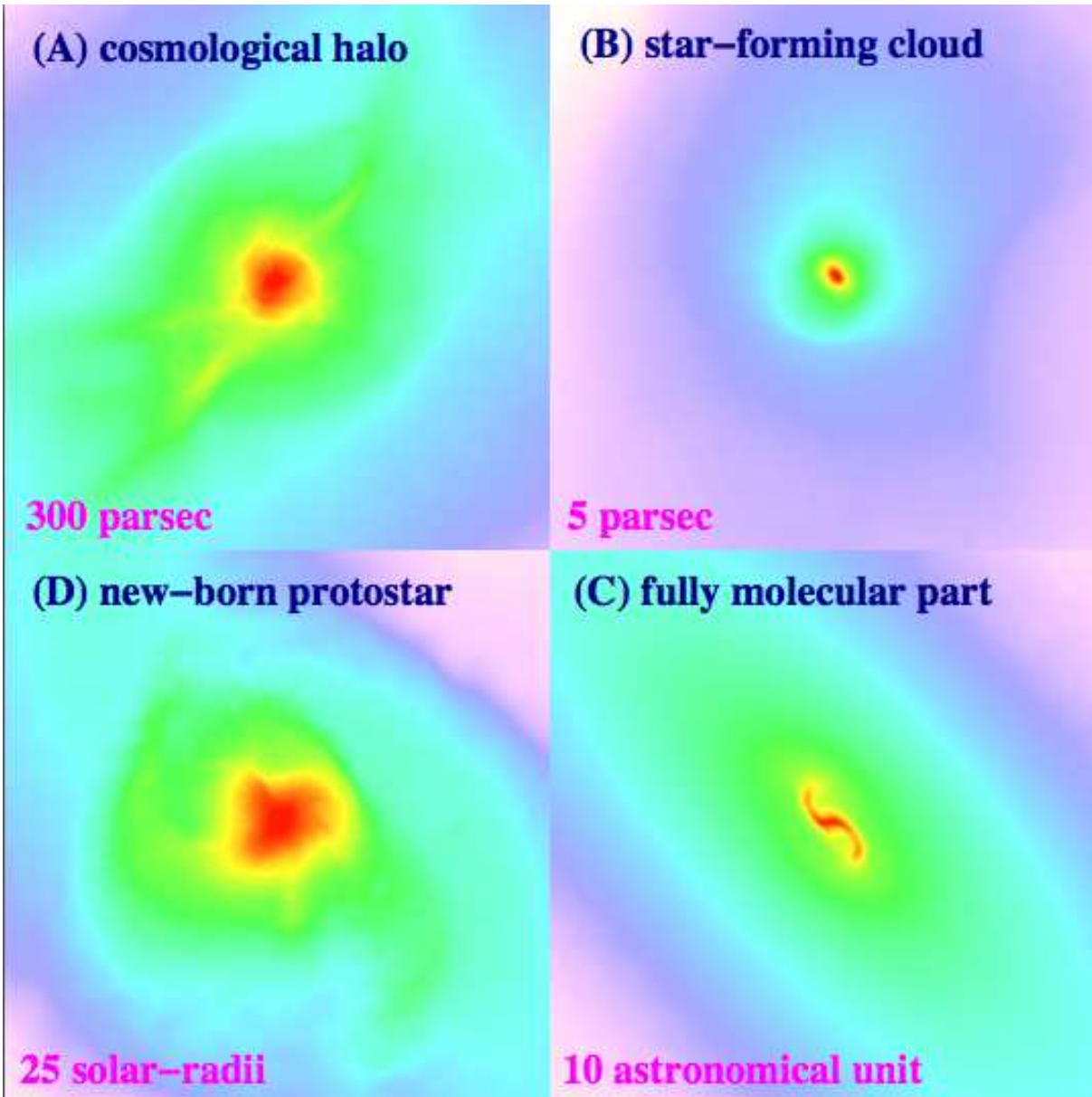


Figure 6: Projected gas distribution around the protostar. Shown regions are, from top-left, clockwise, the large-scale gas distribution around the cosmological halo (300 pc on a side), a self-gravitating, star-forming cloud (5 pc on a side), the central part of the fully molecular core (10 astronomical units on a side), and the final protostar (25 solar-radii on a side). We use the density-weighted temperature to color the bottom-left panel, to show clearly the complex structure of the protostar. From Ref. (34).

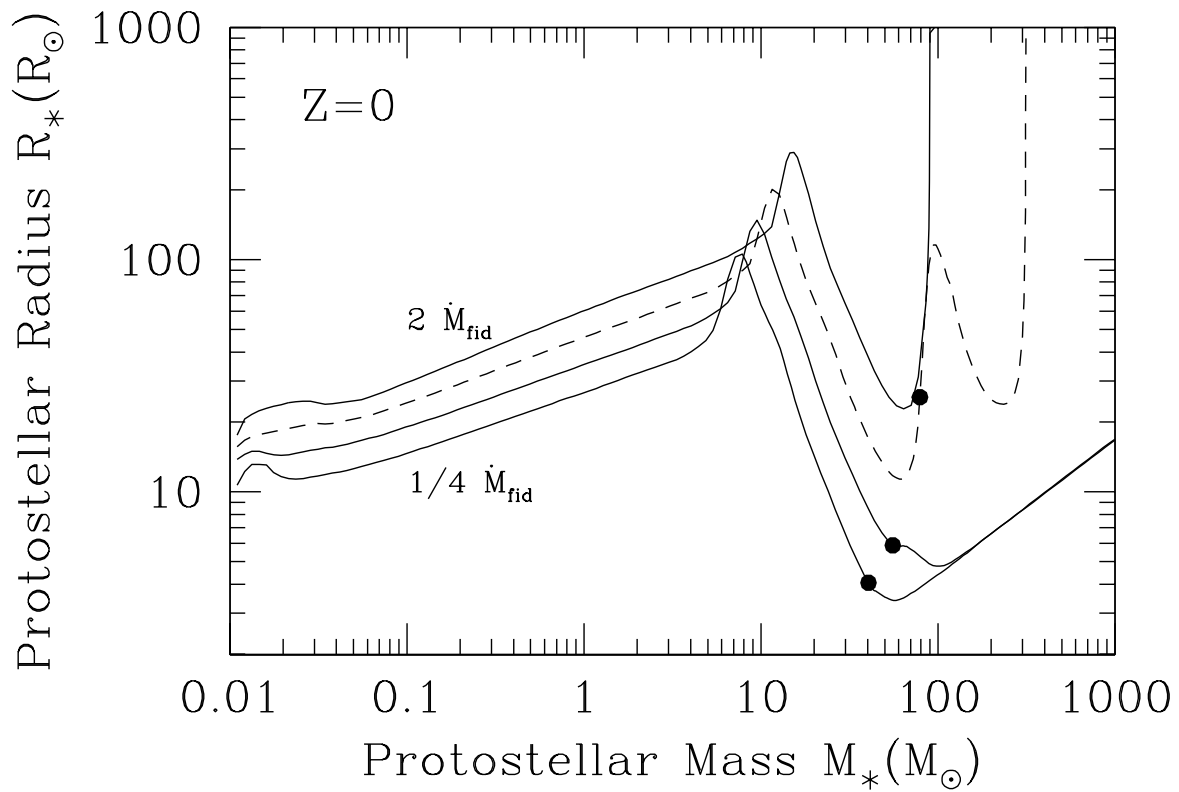


Figure 7: The evolution of the radius and mass of a primordial protostar. The accretion rates assumed are $1/4$, $1/2$, 1 , $2 \dot{M}_{\text{fid}}$ (from bottom to top) with the fiducial rate of $\dot{M}_{\text{fid}} = 4.4 \times 10^{-3} M_{\odot} \text{yr}^{-1}$. The solid points indicate the time when hydrogen burning begins. From Ref. (43).

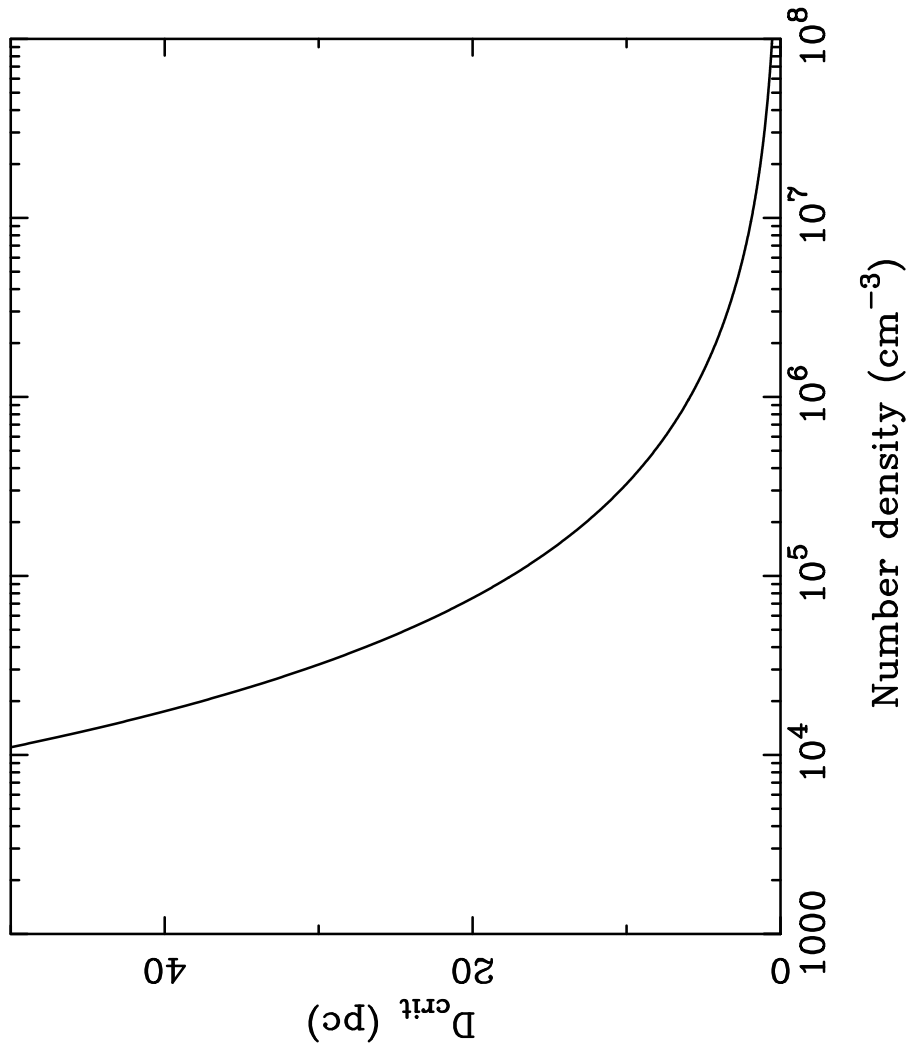


Figure 8: The distance from a radiation source at which the dissociation and free-fall timescales are equal, plotted as a function of gas cloud density. From Ref. (54).

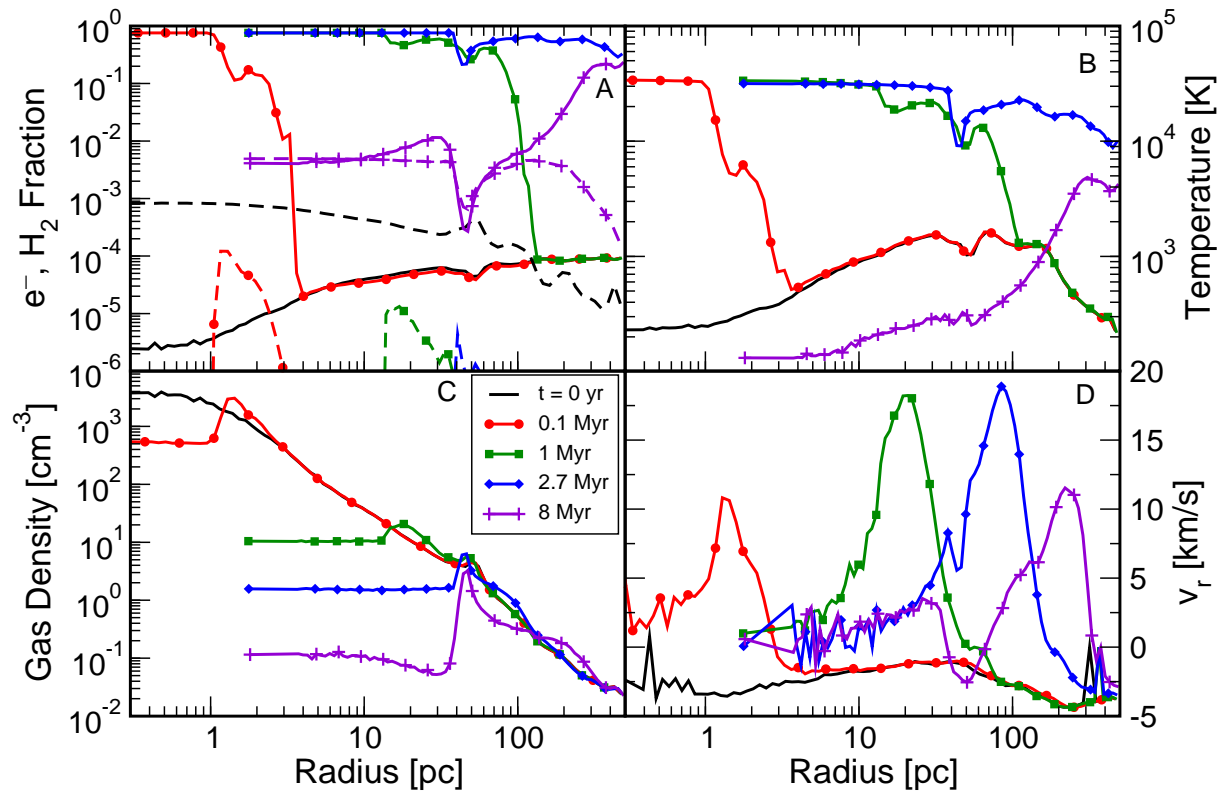


Figure 9: The structure and evolution of an HII region around a massive Population III star inside a minihalo. Radial profiles of ionization fraction, density, temperature, and velocity are plotted for five output times. From Ref. (67)

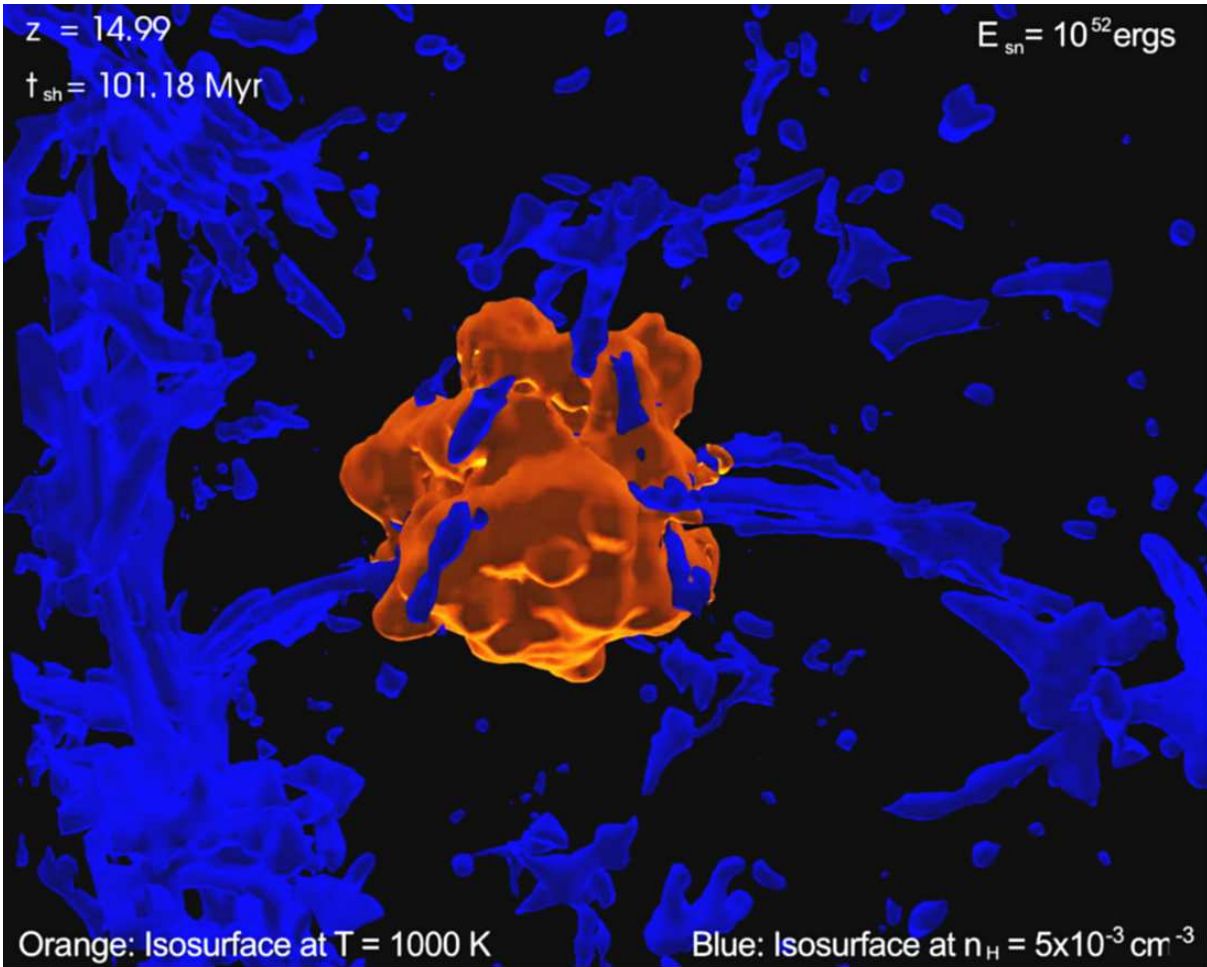


Figure 10: The structure of an early supernova remnant. The shock-front reached a radius of 2 kpc about 100 Myrs after the explosion. A large explosion energy of 10^{52} ergs is assumed for this simulation. From Ref. (82).

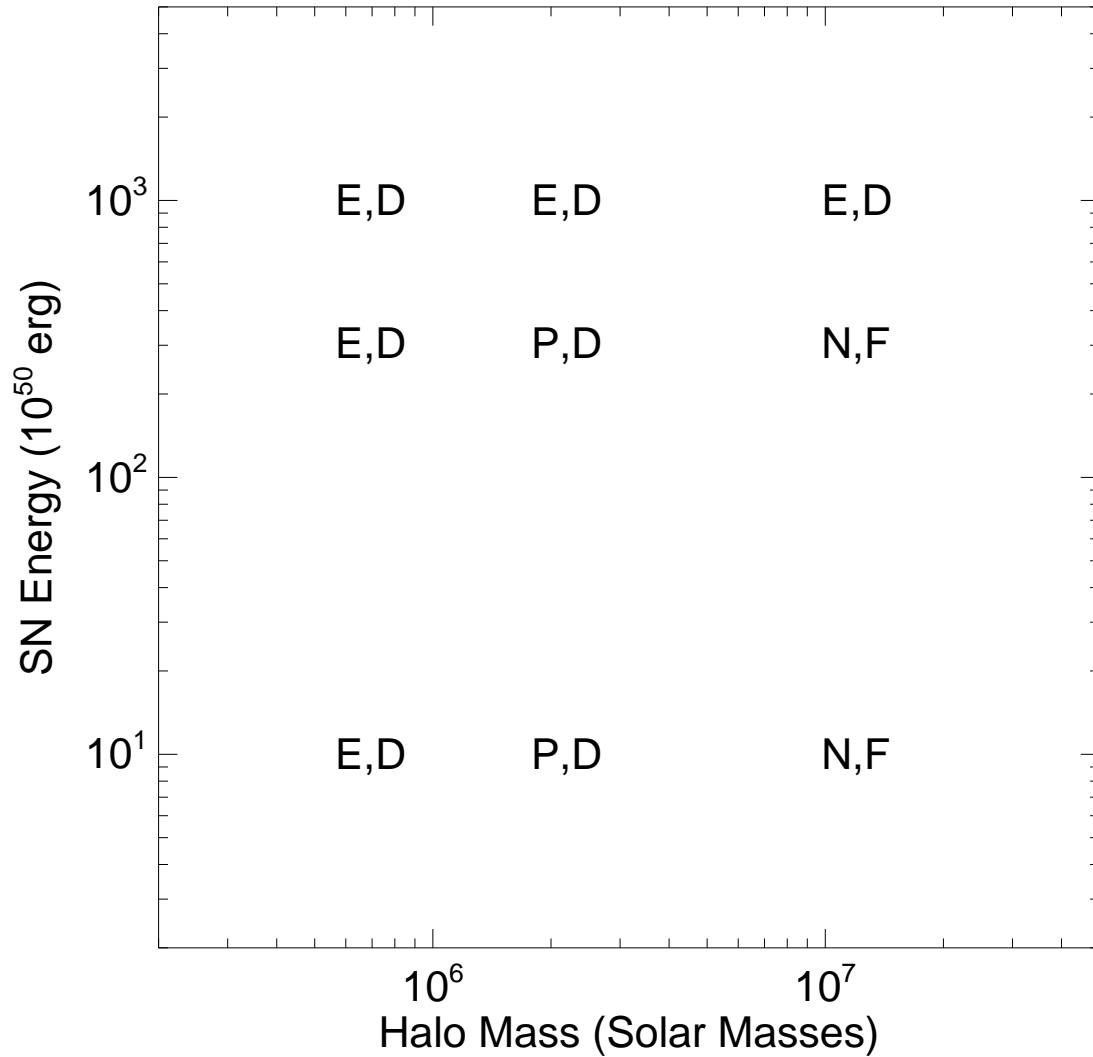


Figure 11: Destruction efficiency of the first supernovae. The first letter refers to the initial state of the halo prior to the explosion; E: photoevaporated; P: partly ionized, defined as the I-front not reaching the virial radius; N: neutral, or a failed HII region. The second letter indicates outcome of the SN explosion; D: destroyed, or F: fallback. From Ref. (73).